Dispensing and surface-induced crystallization of zeptolitre liquid metal-alloy drops

PETER W. SUTTER AND ELI A. SUTTER*

Center for Functional Nanomaterials, Brookhaven National Laboratory, Upton, New York 11973, USA

*e-mail: esutter@bnl.gov

Published online: 15 April 2007; doi:10.1038/nmat1894

The controlled delivery of fluids is a key process in nature and in many areas of science and technology, where pipettes or related devices are used for dispensing well-defined fluid volumes. Existing pipettes are capable of delivering fluids with attolitre (10^{-18} l) accuracy at best[1]. Studies on phase transformations of nanoscale objects would benefit from the controlled dispensing and manipulation of much smaller droplets. In contrast to nanoparticle melting whose fundamental pathway was studied extensively[2], experiments on crystallization, testing classical nucleation theory[3], are hindered by the influence of support interfaces. Experiments on free-standing fluid drops are extremely challenging[4]. Here, we demonstrate the operation of a pipette, which, observed by transmission electron microscopy, delivers a metal-alloy melt with zeptolitre (10^{-21} l) resolution. We use this exquisite control to produce nearly free-standing $Au_{72}Ge_{28}$ drops suspended by an atomic-scale meniscus at the pipette tip, and to image their phase transformations with near-atomic resolution. Our observations of the liquid–solid transition challenge classical nucleation theory[3] by providing experimental evidence for an intrinsic crystallization pathway of nanometre-sized fluid drops that avoids nucleation in the interior, but instead proceeds via liquid-state surface faceting as a precursor to surface-induced crystallization.

The main building blocks and operation of the zeptolitre pipette are shown in Fig. 1. The entire set-up is mounted on the variable-temperature stage of a transmission electron microscope (TEM), which serves to both actuate and observe the operation of the pipette. A germanium nanowire (NW) constitutes the pipette body, providing the mechanical support necessary to hold the pipette tip steady in vacuum (Fig. 1a). The tip itself (Fig. 1b) consists of a reservoir of Au–Ge alloy with a composition close to the eutectic point in the binary phase diagram ($Au_{72}Ge_{28}$ (ref. 5)). The entire NW and the Au–Ge reservoir are encapsulated in a self-assembled multilayer shell of crystalline carbon (Fig. 1c; see ref. 6 and the Methods section for details).

To operate the pipette, the Au–Ge reservoir is melted by heating above the bulk eutectic temperature ($T_E = 361°C$ (ref. 5)), and the expulsion of liquid metal alloy is triggered by opening a small channel (the pipette 'nozzle') in the C-shell by briefly focusing a tight (~1 nm) electron beam onto the shell. An escaping liquid drop is observed outside the shell immediately after returning the TEM to imaging conditions (Fig. 1e). The drop is perfectly spherical and has an initial volume of about 3 zl (diameter ~18 nm). Over several hundred seconds, it slowly grows to over 30 zl in volume. At the same time, the Au–Ge reservoir is shrinking continuously. This process is shown in Fig. 1e–g (see also Supplementary Information movie).

Figure 1d shows the evolution of the drop volume, determined from time-lapse TEM images, for two fluid-delivery experiments from different zeptolitre pipettes. The expelled fluid volume increases with time until, abruptly on a timescale of a few seconds, the drop volume stabilizes and remains constant. With proper definition of the starting time, the growth of both drops is almost identical, suggesting that different pipettes operate reproducibly under similar conditions. In contrast to other studies on liquid metals contained in C, for instance Ga/C nanothermometers in which thermal expansion was used to drive fluid flow inside multiwall C-nanotubes[7], high pressure generated by the C-shell encapsulating the pipette reservoir plays the key role of driving the fluid flow and expulsion in our experiments[8–10]. On the basis of shifts in the melting and crystallization temperatures of nanoparticles of low-melting-point metals (Pb, Sn) encapsulated in comparable multilayer C-shells, typical pressures inside such structures were estimated to be in the GPa range[11]. Observations of our shell structures, a sandwich of wavy graphene sheets with alternating inward and outward curvature (Fig. 1c), suggest that elastic relaxation of the shell can propel the initial fluid flow from the pipette reservoir. Large-scale rearrangements of the C-shell are observed only later, when the rate of fluid expulsion becomes probably determined increasingly by the restructuring of the shell.

When dispensing a small drop into vacuum, the effective driving force for fluid flow is the difference between the reservoir pressure, p_{res}, and the Laplace pressure due to the surface tension, γ, of the spherical drop with radius R: $\Delta p = p_{res} - (2\gamma/R)$. Steady flow can only be established if the reservoir pressure exceeds the Laplace pressure of a small (<10 nm) initial drop, which for liquid metals or alloys (for example, $\gamma(\mathrm{Au}) = 1.169\ \mathrm{N\,m^{-1}}$ at 1,064 °C, ref. 12) can be of the order of 1 GPa. The operation of the pipette can be further analysed using the Hagen–Poiseuille relation, giving the change of fluid volume (V) with time (t), $(\mathrm{d}V/\mathrm{d}t) = (\pi r^4/8\mu\ell)\Delta p$, for the flow rate of a viscous fluid (viscosity, μ), driven through a narrow nozzle (radius, r; length, ℓ) by a pressure difference, Δp.

In contrast to macroscopic flow, the flow through an atomic-scale nozzle may be dominated entirely by fluid–nozzle interactions, that is, the effective viscosity, μ, derived from the above relation will reflect friction in the nozzle rather than a bulk property of the fluid in the reservoir. This picture is indeed

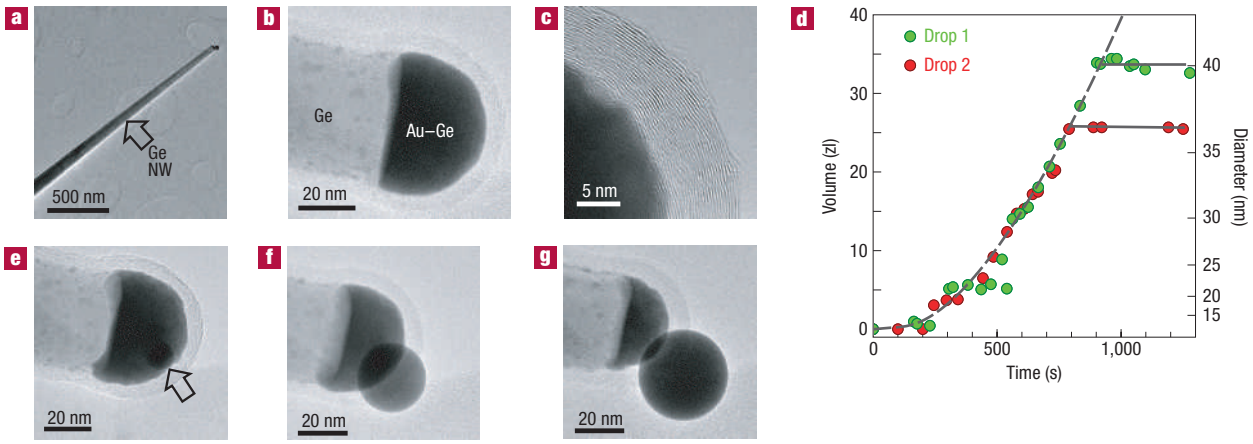

Figure 1 Building blocks and operation of the zeptolitre pipette. a, Ge nanowire pipette body. **b**, Fluid reservoir at the pipette tip, containing a $Au_{72}Ge_{28}$ alloy melt encapsulated into a multilayer carbon shell ($T = 425\,^{\circ}C$). **c**, Interface between the liquid $Au_{72}Ge_{28}$ reservoir and the carbon shell, consisting of multiple curved graphene layers. **d**, Time dependence of the size of the dispensed $Au_{72}Ge_{28}$ drop for two different pipetting experiments. Lines are guides to the eye. **e–g**, Expulsion of a $Au_{72}Ge_{28}$ melt drop during operation of the zeptolitre pipette at 425 °C.

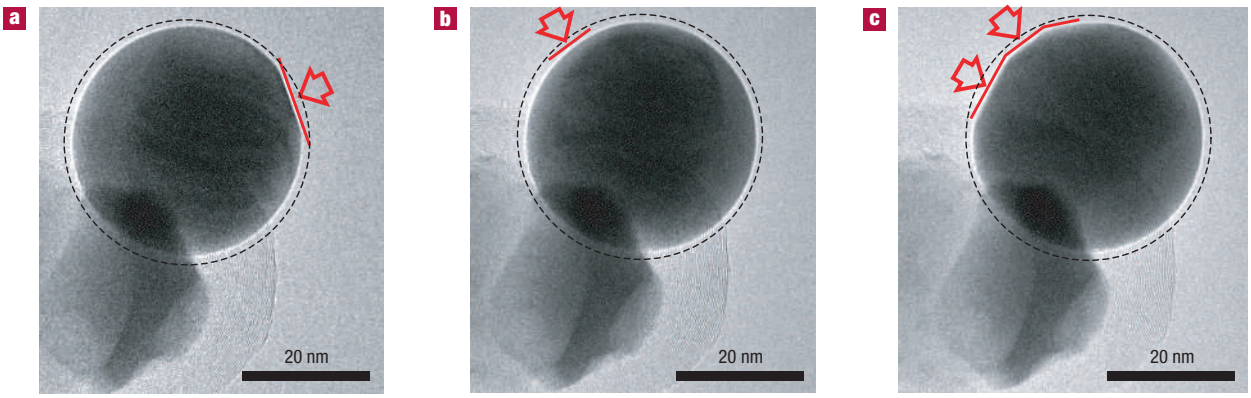

Figure 2 Transient faceting of a 30 nm $Au_{72}Ge_{28}$ drop near the liquid–solid phase transition. a–c, Still images of the same drop at different times, while the temperature is held at $T = 305\,^{\circ}C$. The dashed circles illustrate deviations of the projected drop shape from the spherical shape found at higher temperature. The arrows mark extended planar surface facets.

confirmed by a least-squares fit of the viscous flow relation to the measured drop evolution. For realistic values of nozzle length ($\ell \approx 10$ nm; the measured C-shell thickness) and radius ($r \approx 1$ nm), the fit yields a reservoir pressure $p_{res} = 0.77$ GPa and viscosity $\mu = 7 \times 10^5$ Pa s. The extreme value of μ, several orders of magnitude higher than the bulk viscosity of metallic melts[12] and well beyond the possible range of viscosity under pressure[13], suggests significant wetting-induced dissipative fluid–nozzle interactions. Atomistic simulations of nanoscale fluid jets have indeed predicted strong frictional interactions when wetting is not prevented between a model fluid and the surface of a microscopic ejection nozzle[14]. However, whereas simulations over a few nanoseconds show only two flow regimes—rapid ejection as a jet or complete clogging of the nozzle—our experiments demonstrate an important third regime accessible in practice: the slow, controlled delivery of individual drops with volume in the zeptolitre range.

The zeptolitre pipette can maintain an expelled fluid drop, held only by a thin 'thread' of alloy melt emerging from the nozzle, in a quasi-containerless environment. This unique 'pendant drop' geometry permits the direct microscopic observation of melting and crystallization of individual, free-standing metal-alloy particles containing 10^4–10^6 atoms, a regime in which significant deviations from macroscopic behaviour[15] can be expected, but in which the drops are too large to allow for extended atomistic simulations of their phase behaviour.

We used several zeptolitre pipettes to observe the crystallization of $Au_{72}Ge_{28}$ drops with diameters between 20 and 40 nm. Small alloy volumes of a few tens of zeptolitres show significant hysteresis between melting and crystallization[15]. The melting temperature is size dependent, but generally lies around 350 °C for the particle sizes considered here. Crystallization occurs around 290–300 °C, that is, substantial supercooling is achieved for free-standing drops. During slow cooling, the drops appear as homogeneous spheres without any internal contrast. However, a few degrees Celsius above the crystallization point, the supercooled drops suddenly develop partial surface facets, while remaining perfectly spherical over the remainder of their surface (Fig. 2). Faceted surface segments

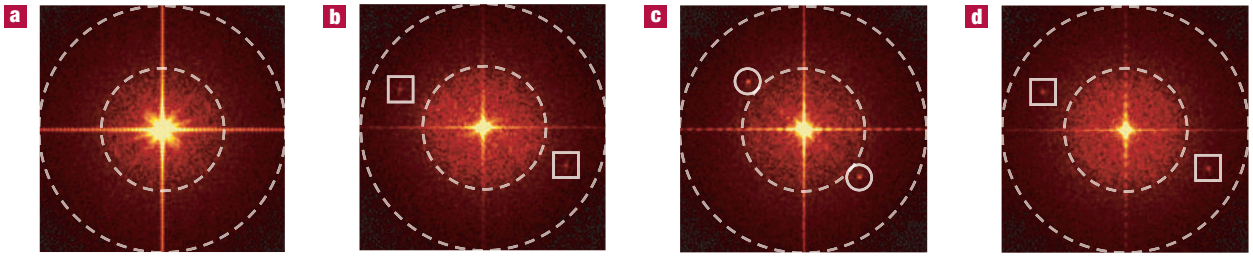

Figure 3 Fourier-transforms (FTs) of selected areas of TEM images in the transient faceting and crystallized states of a zeptolitre $Au_{72}Ge_{28}$ drop. a, FT of the area in Fig. 2a showing the transient faceted drop ($T = 305\,^{\circ}C$). **b**, FT of the adjacent Ge nanowire in the same image (305 °C). **c**, FT of the zeptolitre drop after crystallization (285 °C). **d**, FT of the Ge nanowire (285 °C). The dashed circles indicate spatial frequencies of ($2\pi/0.15$ nm) and ($2\pi/0.3$ nm), respectively. The white squares and circles mark spots arising from Ge(113) fringes (0.191 nm spacing) and Au(111) fringes (0.235 nm), respectively.

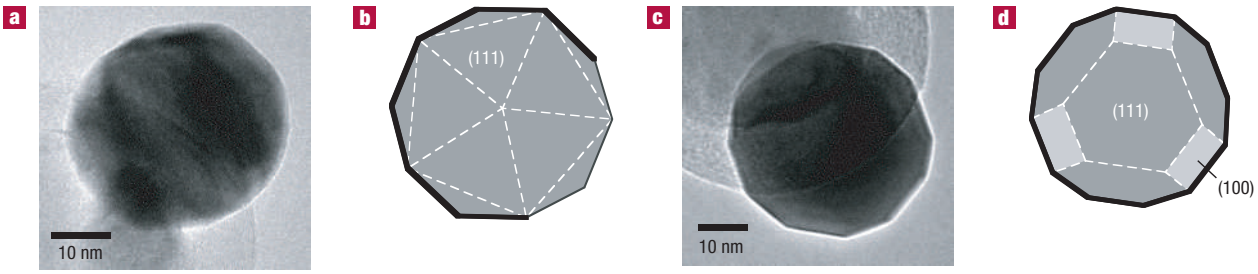

Figure 4 Comparison of frozen-in crystalline shapes of 'free' and 'supported' $Au_{72}Ge_{28}$ clusters. a, TEM image of a crystalline cluster that underwent extensive transient surface faceting in the liquid state. **b**, Projection of the icosahedral motif bounded by (111) facets, oriented to match the facets in the upper left section of the cluster shown in **a**. **c**, Image of a crystalline cluster, which in the liquid state showed wetting interactions with the C-shell at the pipette tip. **d**, Projection of the truncated octahedral (f.c.c.) motif.

continuously form and decay by converting back to the spherical shape. This transient surface faceting could be maintained for several hours with the drop temperature stabilized a few degrees above the point at which crystallization was eventually observed. In this regime, the internal volume clearly remains in the liquid state, showing no change in image contrast compared with the appearance of the same drop at higher temperatures. Fourier-transform analysis of our TEM images confirms the liquid state of drops in the transient faceting regime. Power spectra of image areas containing strongly faceted $Au_{72}Ge_{28}$ drops (such as shown in Fig. 2a) show no distinct reflections that could be associated with crystalline order in the drops (Fig. 3a), whereas clear 'diffraction spots' are invariably observed for the adjacent crystalline Ge nanowire material (Fig. 3b). Once crystallization is induced by lowering the temperature, strong reflections are detected from the solid drops (Fig. 3c), consistent with the spacing of (111) lattice planes in the crystalline AuGe alloy.

Faceting is considered as one of the hallmarks of the crystalline state. Stable facets with low specific surface free energy determine the equilibrium shape of small solid particles, as first shown by Wulff over a century ago[16]. The occurrence of planar facets on a liquid drop is highly unusual, as it requires an anisotropic surface free energy not found in liquids. We conclude that supercooled nanoscale $Au_{72}Ge_{28}$ drops close to crystallization develop some degree of ordering, at least locally in the areas showing transient faceting. An arrangement of near-surface atoms in layers, even without long-range order in the layers, would produce a cusp in the surface energy and would hence be sufficient to induce faceting. Surface layering in liquids, first predicted by Rice *et al.*[17], has been found near macroscopic planar liquid–vapour interfaces of a wide range of metal and alloy melts, including liquid Ga (ref. 18), eutectic BiSn (ref. 19), AuSi (ref. 20) and AuGe (ref. 20). For binary alloys, segregation of the component with lower surface tension to the outermost layers typically accompanies and may consequently affect liquid-state surface layering[19,20]. Layering due to surface compression has been predicted for melts of heavy noble metals, again in a planar geometry[21].

An extended planar liquid surface provides a natural template for surface layering. For layering to occur in a drop, its spherical symmetry needs to be lifted first. Our observations suggest that this process occurs quite readily, probably by small fluctuations of the drop shape creating microscopic planar areas, which then develop into extended facets. The energy cost of forming a planar surface segment on a spherical drop can be estimated as the product of the increase in surface area and the specific surface free energy, γ, of the fluid. The generation of a small planar area, a few nanometres in diameter, on a 30–40 nm drop would increase the surface energy only by about 200 meV, that is, would occur spontaneously at the temperatures considered here. Forming the actual 11-nm-diameter facet shown in Fig. 2a would cause much larger (>10 eV) increases in surface energy, that is, would be exceedingly improbable to occur as a fluctuation but would require additional stabilization, for example, by near-surface layering.

Occurring entirely in the liquid state, the dynamic surface faceting of supercooled drops is clearly distinct from a previously proposed 'quasi-molten' state[22], a liquid–solid transition regime in which a crystalline cluster can fluctuate in time between different structures. We do not observe distinct 'quasi-melting', probably

owing to the large size of our AuGe drops, which would narrow the phase space in which structure fluctuations can occur[22]. In the absence of fluctuations in the solid state, a comparison of the drop shape during transient faceting with the frozen-in shapes of subsequently crystallized clusters can be used to explore the role of transient surface faceting in the crystallization process.

In all cases in which liquid $Au_{72}Ge_{28}$ drops could be maintained in a state of transient surface faceting, a further reduction of the temperature induced freezing into a cluster shape containing large faceted segments that match the projection of an icosahedral cluster (Fig. 4a,b). Surface facets coincide closely with the last set of transient facets present when crystallization was induced (Fig. 2c). On the other hand, suspended drops were occasionally observed to make contact with and wet the carbon shell at the pipette tip. Such drops could not be stabilized in a transient faceted state, and invariably crystallized in a shape closely matching a suitably oriented truncated octahedron, indicative of a face-centred cubic (f.c.c.) cluster (Fig. 4c,d). Given the preference of larger Au nanoclusters for the stable f.c.c. structure[23], the formation of facets with icosahedral symmetry strongly suggests crystallization originating at close-packed (111)-like surface planes, that is, a surface-induced crystallization templated by the transient surface facets of 'free' liquid drops. Conversely, the truncated octahedral shape resulting from the freezing of 'supported' drops is consistent with a crystallization front spreading from a single nucleus, probably at the drop-support interface, and hence producing a monocrystalline f.c.c. cluster.

Our experiments on a specific model system—spherical $Au_{72}Ge_{28}$ drops dispensed from and suspended by zeptolitre pipettes—provide direct microscopic evidence of long-term dynamic surface faceting of supercooled liquid drops, acting as a template for surface-induced crystallization. These findings challenge a key assumption of the accepted theory of crystallization, classical nucleation theory[3]: the concept of a stable nucleus aggregating spontaneously and initiating solidification from the interior of a drop. Qualitatively similar behaviour, albeit on much shorter timescales, has been predicted recently in numerical simulations of the quenching of small Au drops[24]. Ordering effects in the liquid phase that can stabilize large facets on liquid drops, such as near-surface layering, have been found for a wide range of metal and metal-alloy systems. A nucleationless surface crystallization pathway involving liquid-state faceting may therefore govern the crystallization of nanometre-sized metal and metal-alloy drops in general, and possibly the freezing of small drops of a wide range of other fluids.

METHODS

TRANSMISSION ELECTRON MICROSCOPY

All experiments are carried out in a JEOL 3000F field-emission TEM equipped with a Gatan 652 high-temperature specimen holder with a temperature range between room temperature and 1,000 °C. The specimen temperature is measured by a type-R thermocouple (Pt–Pt13%Rh) and is electronically controlled with a stability of about ±1 °C. Specimens consist of Ge nanowires dispersed on ultrathin amorphous carbon films supported by standard copper grids. *In situ* TEM observations are carried out at temperatures up to 500 °C in high vacuum (below 2×10^{-5} Pa), and at electron irradiation intensities during imaging between <2 and up to 50 A cm^{-2}. High-resolution TEM images are recorded electronically using a 1,024 × 1,024 pixel charge-coupled device camera and Gatan Digital Micrograph software.

FABRICATION AND OPERATION OF ZEPTOLITRE PIPETTES

Zeptolitre pipettes are assembled *in situ* in the TEM from Ge NWs grown in an ultrahigh-vacuum environment from germane (GeH_4) on Au catalyst particles dispersed on silicon substrates. At elevated temperature (about 400 °C) and in the presence of carbon (from the amorphous carbon support), the Au in the catalyst particles and small Au aggregates on the NW surface drive the complete encapsulation of the NW and Au-rich tip into a multilayer shell of graphene fragments (see ref. 6 for details). This process produces a pipette reservoir consisting of a Au–Ge alloy in contact with a crystalline Ge NW, and surrounded by a graphitic carbon shell. Annealing at temperatures above the eutectic temperature (400−420 °C) of a bulk Au–Ge binary alloy is used to adjust the Ge concentration in the reservoir. *In situ* energy-dispersive X-ray spectroscopy analysis (measured after cooling to room temperature) confirmed compositions of the alloy melt in the reservoir and of the expelled drop very close to the Au–Ge eutectic composition (28 atomic % Ge). Electron irradiation is used to tighten the curved carbon shell and build up pressure on the pipette reservoir[9].

With the sample held at the same temperature (liquid Au–Ge alloy in the pipette reservoir), the electron beam is focused into a tight spot below 1 nm in diameter for a fraction of a second, which opens a channel in the tip and triggers the expulsion of a melt drop. The further dispensing of the drop is imaged by TEM at low electron intensity (<2 A cm^{-2}).

FITTING OF THE MEASURED DROP SIZE EVOLUTION

From time-lapse TEM images of drop expulsion, $R_{\mathrm{Drop}}(t)$ was determined and the expulsion rate $\mathrm{d}V/\mathrm{d}t$ computed as a function of drop radius. A least-squares fit of the early-stage $\mathrm{d}V/\mathrm{d}t(R)$ to the Hagen–Poiseuille equation, $(\mathrm{d}V/\mathrm{d}t) = (\pi r^4/8\mu\ell)(p_{\mathrm{res}} - (2\gamma/R))$, was carried out for fixed surface tension $\gamma = 1$ N m^{-1}. A best fit to the experimental data was obtained for reservoir pressure $p_{\mathrm{res}} = 7.7 \times 10^8$ Pa and viscosity $\mu = 8 \times 10^5$ Pa s.

Received 9 January 2007; accepted 23 March 2007; published 15 April 2007.

References

1. Meister, A., Liley, M., Brugger, J., Pugin, R. & Heinzelmann, H. Nanodispenser for attoliter volume deposition using atomic force microscopy probes modified by focused-ion-beam milling. *Appl. Phys. Lett.* **85**, 6260–6262 (2004).
2. Frenken, J. W. M. & van der Veen, J. F. Observation of surface melting. *Phys. Rev. Lett.* **54**, 134 (1985).
3. Volmer, M. *Kinetik der Phasenbildung* (Steinkopff, Leipzig, 1939).
4. Egry, I., Lohoefer, G. & Jacobs, G. Surface tension of liquid metals: Results from measurements on ground and in space. *Phys. Rev. Lett.* **75**, 4043 (1995).
5. Predel, B. in *Crystallographic and Thermodynamic Data of Binary Alloys—Electronic Materials and Semiconductors* (ed. Madelung, O.) (Landolt-Bornstein, Group IV: Physical Chemistry, Vol. 5, Springer, Berlin, 1998).
6. Sutter, E. & Sutter, P. Au-induced encapsulation of Ge nanowires in protective carbon shells. *Adv. Mater.* **18**, 2583 (2006).
7. Gao, Y. & Bando, Y. Carbon nanothermometer containing gallium. *Nature* **415**, 599 (2002).
8. Sun, L. *et al.* Carbon nanotubes as high-pressure cylinders and nanoextruders. *Science* **312**, 1199–1202 (2006).
9. Banhart, F. Irradiation effects in carbon nanostructures. *Rep. Prog. Phys.* **62**, 1181–1221 (1999).
10. Sutter, E., Sutter, P. & Zhu, Y. Assembly and interaction of Au/C core-shell nanostructures: In situ observation in the transmission electron microscope. *Nano Lett.* **5**, 2092–2096 (2005).
11. Banhart, F., Hernández, E. & Terrones, M. Extreme superheating and supercooling of encapsulated metals in fullerenelike shells. *Phys. Rev. Lett.* **90**, 185502 (2003).
12. Iida, T. & Guthrie, R. I. L. *The Physical Properties of Liquid Metals* (Clarendon, Oxford, 1988).
13. Schmelzer, J. W., Zanotto, E. D. & Fokin, V. M. Pressure dependence of viscosity. *J. Chem. Phys.* **122**, 074511 (2005).
14. Moseler, M. & Landman, U. Formation, stability, and breakup of nanojets. *Science* **289**, 1165 (2000).
15. Turnbull, D. & Cech, R. E. Microscopic observation of the solidification of small metal droplets. *J. Appl. Phys.* **21**, 804 (1950).
16. Wulff, G. Zur frage der geschwindigkeit des wachstums und der auflösung der kristallflächen. *Z. Kristall. Mineral.* **34**, 449 (1901).
17. Rice, S. A., Guidotti, D., Lemberg, H. L., Murphy, W. C. & Bloch, A. N. in *Advances in Chemical Physics XXVII* (eds Prigogine, I. R. & Rice, S. A.) (Wiley, Chichester, 1974); D'Evelyn, M. P. & Rice, S. A. A study of the liquid-vapor interface of mercury: Computer simulation results. *J. Chem. Phys.* **78**, 5225 (1983).
18. Regan, M. J. *et al.* Surface layering in liquid gallium: An x-ray reflectivity study. *Phys. Rev. Lett.* **75**, 2498 (1995).
19. Shpyrko, O. G. *et al.* Atomic-scale surface demixing in a eutectic liquid BiSn alloy. *Phys. Rev. Lett.* **95**, 106103 (2005).
20. Shpyrko, O. G. *et al.* Surface crystallization in a liquid AuSi alloy. *Science* **313**, 77–80 (2006).
21. Celestini, F., Ercolessi, F. & Tosatti, E. Can liquid metal surfaces have hexatic order? *Phys. Rev. Lett.* **78**, 3153 (1997).
22. Ajayan, P. M. & Marks, L. D. Quasimelting and phases of small particles. *Phys. Rev. Lett.* **60**, 585 (1988).
23. Cleveland, C. L. *et al.* Structural evolution of smaller gold nanocrystals: The truncated decahedral motif. *Phys. Rev. Lett.* **79**, 1873 (1997).
24. Nam, H.-S., Hwang, N. M., Yu, B. D. & Yoon, J.-K. Formation of an icosahedral structure during the freezing of gold nanoclusters: Surface-induced mechanism. *Phys. Rev. Lett.* **89**, 275502 (2002).

Acknowledgements

This work was carried out under the auspices of the US Department of Energy, under contract No. DE-AC02-98CH1-886.
Correspondence and requests for materials should be addressed to E.A.S.
Supplementary Information accompanies this paper on www.nature.com/naturematerials.

Competing financial interests

The authors declare no competing financial interests.